

# Ecological Environment Changes of Mining Areas Around Nansi Lake With Remote Sensing Monitoring

**Hu Liu**

Shandong University of Science and Technology

**Yan Jiang**

Shandong University of Science and Technology

**Rafal Misa**

Polish Academy of Sciences

**Junhai Gao**

China Coal Technology and Engineering Group Corp Tangshan Research Institute Co., Ltd

**Mingyu Xia**

Shandong University of Science and Technology

**Axel Preusse**

RWTH Aachen University

**Anton Sroka**

Polish Academy of Sciences

**Yue Jiang** (✉ [jiangyue@cumt.edu.cn](mailto:jiangyue@cumt.edu.cn))

China University of Mining and Technology <https://orcid.org/0000-0002-5606-7138>

---

## Research Article

**Keywords:** Nansi lake, Coal mining, Mine ecological environment, Remote sensing monitoring, Environmental change

**Posted Date:** February 16th, 2021

**DOI:** <https://doi.org/10.21203/rs.3.rs-186720/v1>

**License:** © ⓘ This work is licensed under a Creative Commons Attribution 4.0 International License.

[Read Full License](#)

---

**Version of Record:** A version of this preprint was published at Environmental Science and Pollution Research on April 12th, 2021. See the published version at <https://doi.org/10.1007/s11356-021-13849-y>.



30 **Introduction**

31 Nansi lake is located in the southwest of Shandong Province, China (34°27'N to 35°20'N and  
32 116°34'E to 117°24'E), which is composed of Nanyang lake, Dushan lake, Zhaoyang lake, and Weishan  
33 lake. Nansi lake is the largest freshwater lake in Shandong Province and the sixth-largest freshwater  
34 lake in China (the water area is 1266 km<sup>2</sup>). Also, the northern terrain of Nansi lake is higher than the  
35 southern terrain, the length is 125 km from north to south, the width is 5.6 to 30 km from east to west,  
36 the average water depth is 1.5m, and the maximum water depth is 6m. Nansi lake lies within a warm  
37 temperate humid monsoon climate (Liang 2014), which benefits a diversity of plant and animal species  
38 including 539 species of vascular plants, 337 species of vertebrates, and 221 species of birds in the  
39 lake area. Moreover, the lake area is an important habitat and breeding place for many rare and  
40 endangered birds, as well as an important migration and resting place for migratory birds in spring and  
41 autumn. Moreover, Nansi lake was established as a provincial nature reserve by the government in  
42 2003, and then the government adjusted the scope and functional areas of the Nansi lake provincial  
43 nature reserve in 2019 (Fig. 1). The current area is larger than the original after adjustment, the total  
44 area is 1116.51 km<sup>2</sup> and the core zone is 451.15 km<sup>2</sup>, which accounts for 40.41% of the total area.

45

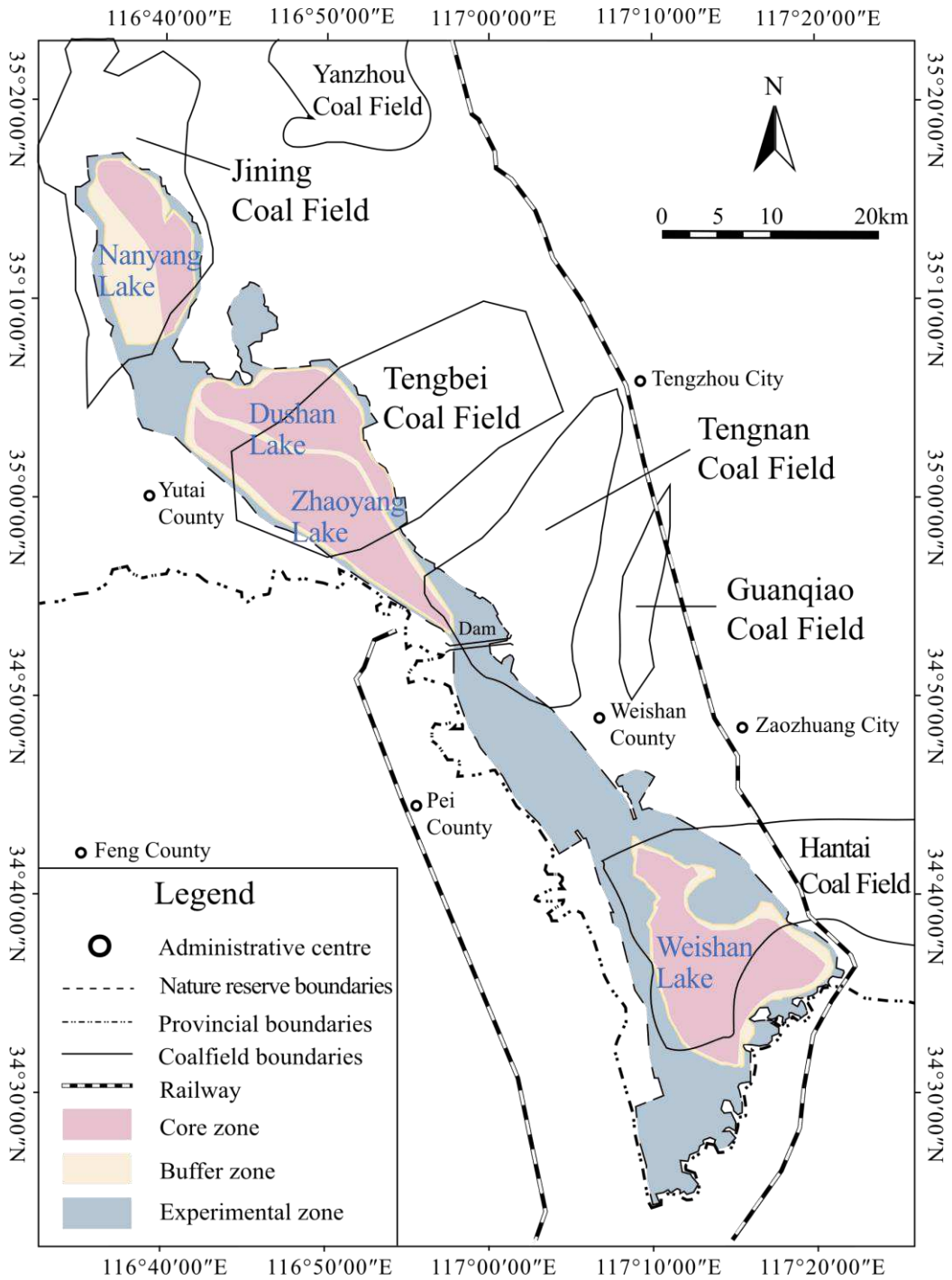


**Fig. 1 Distribution of Nansi lake nature reserve and coal resources**

46

47

48

49

50

51

52

53

Abundant coal resources exist around the Nansi lake area, and people mine coal resources for more than 100 years. In the past two decades, the lake area has been an important energy production base, the coal production accounts for 15% of the total coal production in Shandong Province. The underground mining can destroy the original strata stress balance, which leads to the collapse, fracture, and bending from the bottom to the top. The surface can subside due to the underground mining

54 influence (Den et al. 2015; Jiang et al. 2019). There is a long history of the impact of surface subsidence  
55 on the land environment (Kratzsch 1974; Reddish and Whittaker 1989). However, the research of  
56 water ecological environment damage caused by underground mining is insufficient. Most researches  
57 believe the two viewpoints: (1) Underground mining can not cause surface water to leak into the mine,  
58 and underground mining has no direct impact on surface water; (2) The subsidence caused by mining  
59 can increase the water depth, expand the water storage capacity, decrease the speed of sediment  
60 siltation, and also benefit for irrigation, shipping, aquaculture, etc. (Ma et al. 2019; Shu 1992; Zhang  
61 et al. 2018). The surface subsidence can change the original topography of the lake area and the  
62 ecological environment (a non-pollution hazard to the lake area ecology). On the one hand, researchers  
63 always concentrate on the safeguard of coal mine and maximum utilization of coal resource and form  
64 mature safety measures for underwater mining (Teng et al. 2012). On the other hand, researchers focus  
65 on the destruction law of strata (Sui and Xu 2013; Xu and Sui 2013), but they hardly consider the  
66 impact of underground mining on the ecological environment. However, environmental supervision  
67 departments pay attention to gangue and mine water discharge (Wang et al. 2016) and hardly focus on  
68 the relationship between coal mining and the water ecosystem. At present, the ecological effect of coal  
69 mining on the environment of Nansi lake is not clear, so it is necessary to research this issue.

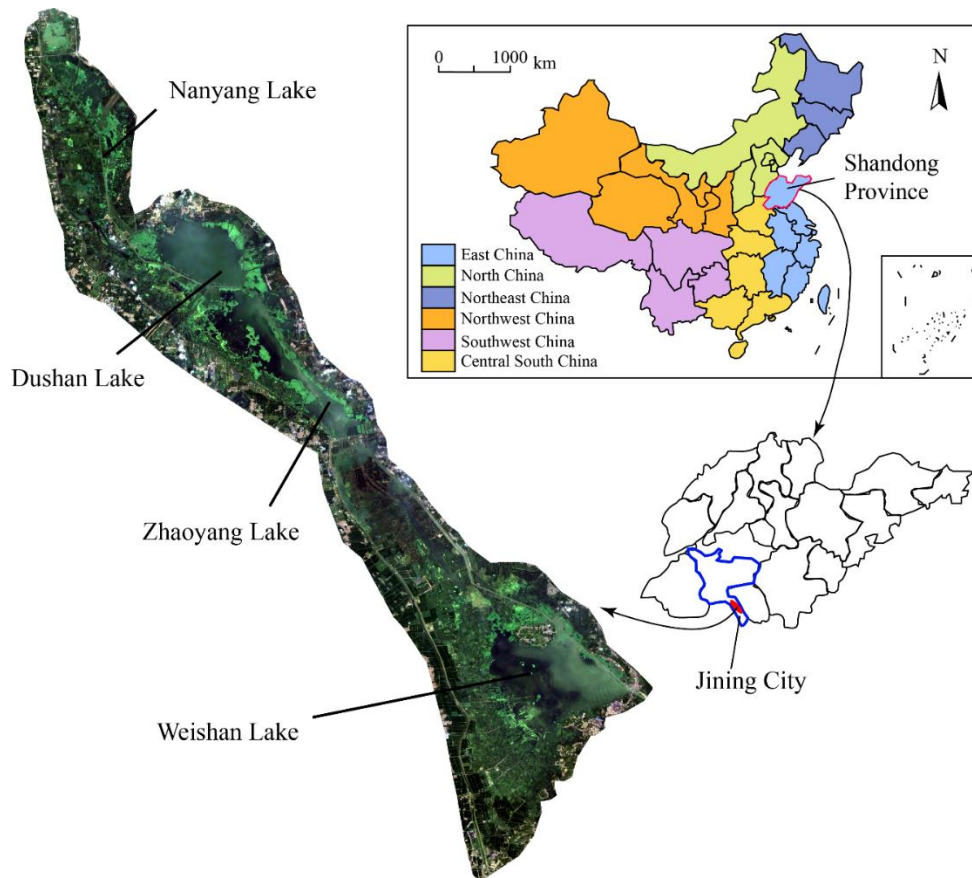
70 The surface subsidence caused by coal mining is a time process, so the impact of mining  
71 subsidence on the environment is a cumulative process, which can not be found in a short time.  
72 Therefore, the long-term remote sensing data from 1988 to 2019 are used to assess the ecological  
73 environment quality of the lake area with the Remote Sensing Ecological Index (RSEI). The  
74 cumulative influence of coal mining on the ecological environment can be indirectly reflected. Finally,  
75 it provides a quantitative scientific basis for evaluating the impact of coal mining on Nansi lake.

76

## 77 **Materials and methods**

### 78 **Research area**

79 Nansi lake is divided into upstream lake and downstream lake by the dam. The research area is  
80 located in the upstream lake that is composed of three lakes (Nanyang lake, Dushan lake, and Zhaoyang  
81 lake) (Fig. 2). The coal-bearing area in the lake is 1789 km<sup>2</sup>, and the average thickness is 11m (Li and  
82 Jiang 2003). More than 40 mines exist in Nansi lake after decades of exploration and development,  
83 Jining, Tengnan, and Tengbei coal fields are located in the research area.



85  
86 **Fig. 2 Location of Nansi Lake (2019 Landsat-8 OLI image)**

87

### 88 **Data acquisition and preprocessing**

89 The main data sources are the Landsat series of remote sensing images, which are freely obtained  
 90 from the U.S. Geological Survey (<https://earthexplorer.usgs.gov/>), Landsat-5 TM data are from  
 91 1988~2005, 2010, and 2011; Landsat-7 ETM data are from 2006~2009; Landsat-8 OLI/TIRS data are  
 92 from 2012, and 2013~2019. The time of these images is selected in August or September due to less  
 93 cloud cover and fair weather. Generally, the recent images (2019) are chosen to be the registration  
 94 benchmark, and the accuracy is controlled within 0.5 pixels. Finally, pretreatments such as radiometric  
 95 calibration, atmospheric correction, and image cropping are implemented.

96

### 97 **Extraction of water area**

98 Support Vector Machine (SVM) classifier is used to extract the upstream lake water area of Nansi  
 99 lake. Compared with other automatic extraction methods of single band threshold, the SVM  
 100 classification method can sufficiently apply the abundant spectral information and geometric texture

101 information, and the extraction accuracy of the water body is higher than that of other methods. SVM  
102 is a kind of generalized linear classifier with a binary classification of supervised learning (Gold and  
103 Sollich 2003). It is widely used in remote sensing image classification and other information extraction.  
104 The classification principle is that apply a hyperplane as the decision boundary, which can achieve  
105 correct classification and maximize the classification interval.

106 The SVM classification method mainly uses two bands of remote sensing data to extract water:  
107 (1) the near-infrared band (0.76~0.90  $\mu\text{m}$ ), in the strong absorption zone of the water body, which is  
108 applied to define the water boundary, and identify the geological structure and landform related to  
109 water; (2) the far-infrared band (2.08~2.35  $\mu\text{m}$ ), in the strong absorption zone of the water body, the  
110 water area appears black in this band. In addition, SVM also combines texture information to  
111 distinguish the boundaries of the lake, fish ponds, and paddy fields. The overall accuracy of  
112 classification is 85%, and the kappa coefficient (an index to measure the accuracy of classification, it  
113 has five different levels to define uniformity, the result is almost perfect between 0.81 and 1.0) is 0.82.  
114 This result illustrates SVM is significant and high precision for extracting lake water area.

115

### 116 **Construction of Remote Sensing Ecology Index (RSEI)**

117 The Ministry of Environmental Protection of China promulgated the latest revision of the  
118 *Technical Criterion for Ecosystem Status Evaluation* (China MEE 2015) in March 2015. The  
119 Ecological Index (EI) from this criterion has five evaluating indicators including biological richness,  
120 vegetation coverage, water network density, land degradation, and pollution load. The indicators of  
121 biological richness, vegetation coverage, water network density can be obtained easily by remote  
122 sensing, but the last two indicators are more difficult to gain by remote sensing. Besides, the weights  
123 of the five indicators are determined by a human, which has a certain subjective deviation. However,  
124 Remote Sensing Ecology Index (RSEI) applies four indicators of greenness, humidity, dryness, and  
125 heat to define the weight of each indicator with principal component analysis, and RSEI can avoid  
126 human subjective deviation. The greenness is similar to the biological richness, vegetation coverage  
127 from the criterion due to the similar calculation method. Humidity is similar to water network density,  
128 it can represent not only lakes and rivers but also the humidity of vegetation and soil. Dryness is related  
129 to land degradation, so the bare soil can express dryness. The higher value of bare soil shows more  
130 serious land degradation. The surface temperature (heat) is related to urban expansion and other

131 environmental changes.

132 Remote Sensing Ecological Index (RSEI) applies to perform principal component analysis (PCA)  
133 for the four components of wetness (Wet), greenness (FVC), dryness (NDBSI), and heat (LST), and  
134 then the first principal component (PC1) is normalized to generate RSEI. PCA is a statistical analysis  
135 method in which multiple variables convert to minorities of principal components with dimensionality  
136 reduction technology (Du and Fowler 2007). These principal components can reflect most of the  
137 information of the original variables, and they are usually expressed as some linear combination of the  
138 original variables.

139 Greenness (FVC): Fractional Vegetation Cover (FVC) refers to the percentage of the vertical  
140 projection area of vegetation on the ground (including leaves, stems, and branches) in a unit area to  
141 the total area of the statistical area (Zhou et al. 2006). Therefore, FVC can be used to indicate the  
142 greenness:

143

$$FVC = \frac{NDVI - NDVI_{soil}}{NDVI_{veg} - NDVI_{soil}} \quad (1)$$

$$NDVI = (\rho_{NIR} - \rho_R) / (\rho_{NIR} + \rho_R) \quad (2)$$

144

145 where

146  $NDVI$ - normalized vegetation index;  $NDVI_{soil}$ -  $NDVI$  value of bare soil or no vegetation cover area;  
147  $NDVI_{veg}$ - the  $NDVI$  value of the vegetation cover area;  $\rho_{NIR}$ - spectral reflectance of the near-infrared  
148 band;  $\rho_R$ - spectral reflectance of the red band

149

150 Wetness (Wet): the wetness index reflects the humidity of water, soil, and vegetation, which is  
151 closely related to the ecological environment (Crist 1985; Huang et al. 2002; Todd and Hoffer 1998).  
152 The Landsat-5 TM data, Landsat-7 ETM data, and Landsat-8 OLI/TIRS data can be respectively  
153 calculated by equation (3), (4), and (5).

154

$$Wet = 0.0315\rho_B + 0.2021\rho_G + 0.3102\rho_R + 0.1594\rho_{NIR} - 0.6806\rho_{SWIR_1} - 0.6109\rho_{SWIR_2} \quad (3)$$

$$Wet = 0.2626\rho_B + 0.2141\rho_G + 0.0926\rho_R + 0.0656\rho_{NIR} - 0.7629\rho_{SWIR_1} - 0.5388\rho_{SWIR_2} \quad (4)$$

$$Wet = 0.1511\rho_B + 0.1973\rho_G + 0.3283\rho_R + 0.03407\rho_{NIR} - 0.7117\rho_{SWIR_1} - 0.4559\rho_{SWIR_2} \quad (5)$$

155

156 where

157  $\rho_B$ - spectral reflectance of the blue band;  $\rho_G$ - spectral reflectance of the green band;  $\rho_R$ - spectral

158 reflectance of the red band;  $\rho_{NIR}$ - spectral reflectance of the near-infrared band;  $\rho_{SWIR_1}$ - spectral

159 reflectance of the mid-infrared band;  $\rho_{SWIR_2}$ - spectral reflectance of the far-infrared band

160

161 Dryness (NDBSI): the dryness index consists of the average of the building index (IBI) (Xu 2008)

162 and the bare soil index (SI) (Rikimaru et al. 2002):

163

$$NDBSI = \frac{IBI + SI}{2} \quad (6)$$

$$IBI = \frac{\frac{2\rho_{SWIR_1}}{\rho_{SWIR_1} + \rho_{NIR}} - \frac{\rho_{NIR}}{\rho_{NIR} + \rho_R} + \frac{\rho_G}{\rho_G + \rho_{SWIR_1}}}{\frac{2\rho_{SWIR_1}}{\rho_{SWIR_1} + \rho_{NIR}} + \frac{\rho_{NIR}}{\rho_{NIR} + \rho_R} + \frac{\rho_G}{\rho_G + \rho_{SWIR_1}}} \quad (7)$$

$$SI = \frac{(\rho_{SWIR_1} + \rho_R) - (\rho_{NIR} + \rho_B)}{(\rho_{SWIR_1} + \rho_R) + (\rho_{NIR} + \rho_B)} \quad (8)$$

164

165 Where

166  $\rho_B$ - spectral reflectance of the blue band;  $\rho_G$ - spectral reflectance of the green band;  $\rho_R$ - spectral

167 reflectance of the red band;  $\rho_{NIR}$ - spectral reflectance of the near-infrared band;  $\rho_{SWIR_1}$ - spectral

168 reflectance of the mid-infrared band

169

170 Heat (LST): The heat index is expressed by the land surface temperature (LST), and its

171 calculation model (Nichol 2005) is following:

172

$$LST = T / [1 + (\lambda T / \rho) \ln \varepsilon] \quad (9)$$

$$T = K_2 / \ln(K_1 / L_{TIR} + 1) \quad (10)$$

173

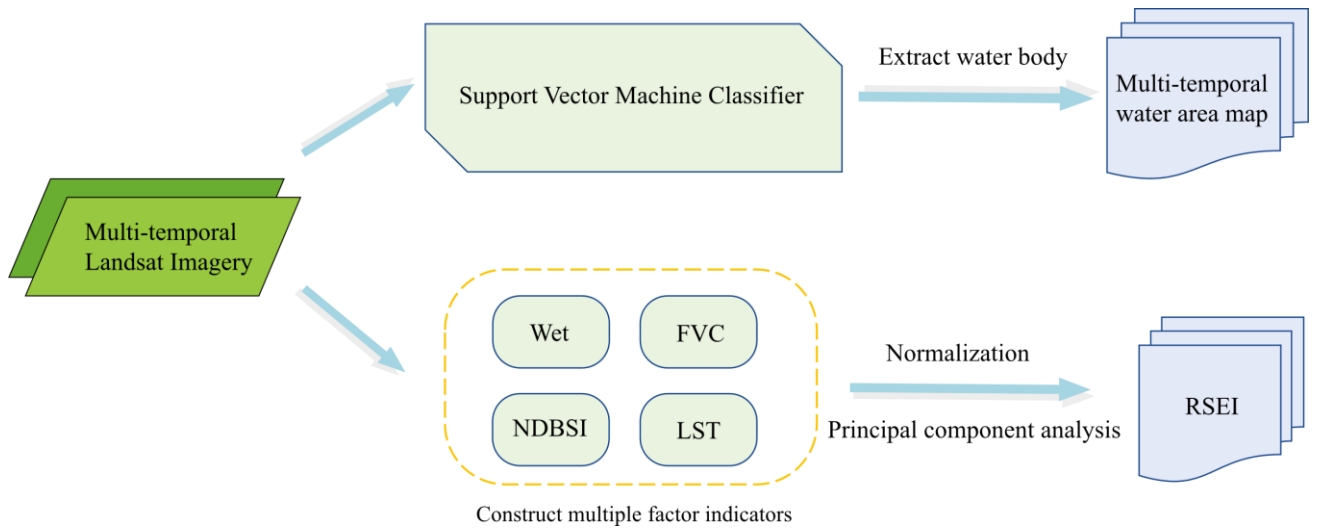
174 where

175  $LST$ - land surface temperature;  $T$ - temperature of the sensor,  $\lambda$ - central wavelength of the thermal  
 176 infrared band;  $\rho$ - calculation parameter ( $1.438 \times 10^{-2} \text{m} \cdot \text{K}$ );  $\varepsilon$ - land surface emissivity (it can be  
 177 calculated by NDVI with Sobrino's model) (Sobrino et al. 2004);  $L_{TIR}$ - the radiation of TM, ETM, and  
 178 TIRS thermal infrared band;  $K_1$  and  $K_2$ - calibration parameters

179

180 Because the dimensions of the four indicators are not uniform, these indicators should be  
 181 standardized before the principal component analysis (Fig. 3). The RSEI result shows the larger value,  
 182 the better the ecological quality.

183



184

185

**Fig. 3 Research method route**

186

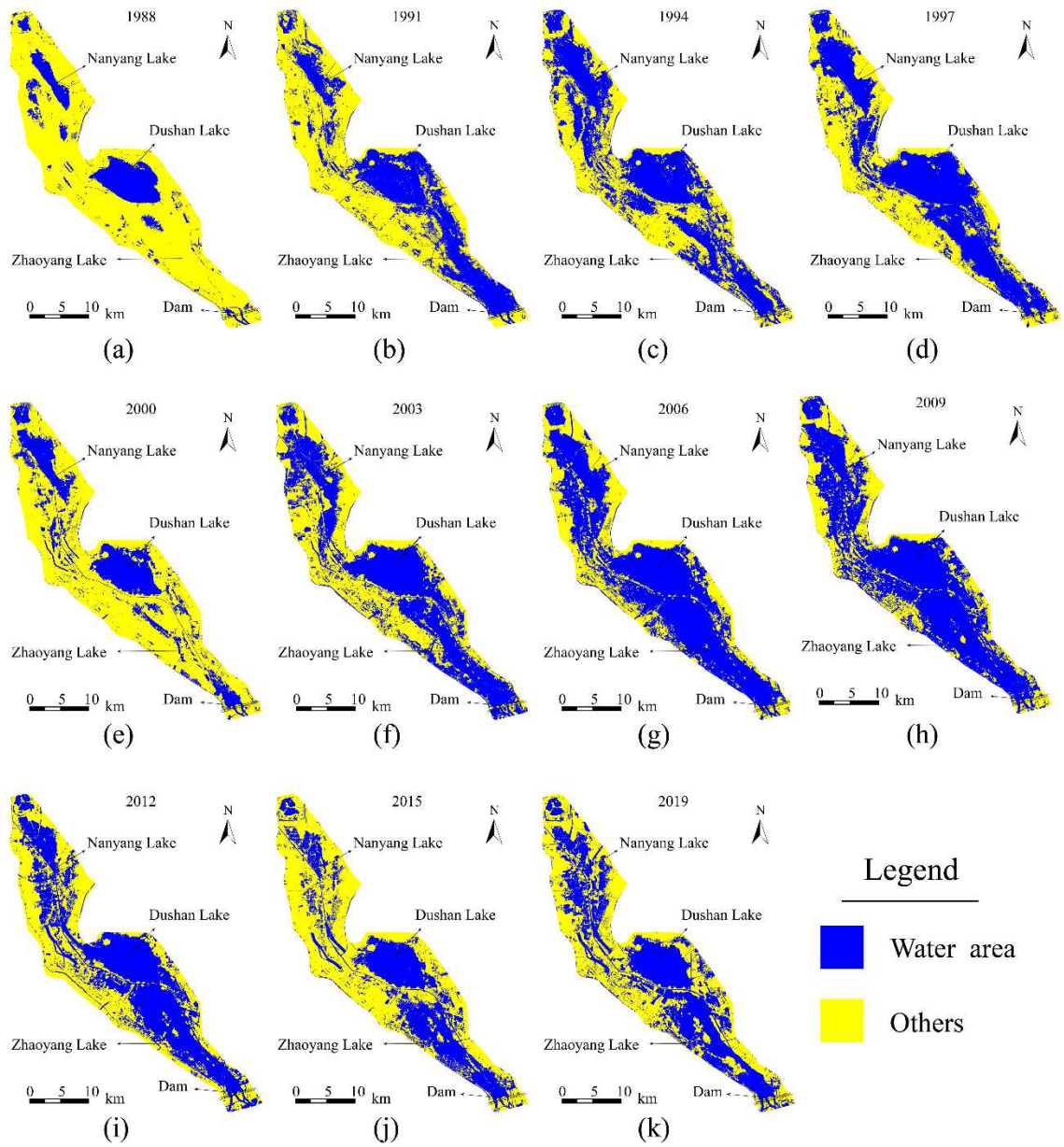
## 187 Results and discussion

### 188 Water area change

189 The SVM classification method was used to extract the water area of upstream Nansi lake from  
 190 1988 to 2019 (Fig. 4). According to the change information of remote sensing monitoring, the water  
 191 areas (blue parts) in 1988 and 2000 were extremely smaller than that of other years (Fig. 4a and 4e),  
 192 Nanyang and Zhaoyang lakes almost dried up due to severe drought from 1987 to 1989 and 2000 to  
 193 2002 (Meng and Dong 2019). The water level of the upstream lake dropped to the lowest level in  
 194 history, and the lake water basically dried up. The water areas decreased every year and appeared

195 fragmented shapes around the lake boundary.

196



197

198

199

**Fig. 4 Variation characteristics of the upstream Nansi lake**

200 In addition, extracted water area data and average precipitation (from 1988 to 2019) were used to  
201 objectively assess the water area change. The trends of water area change (red line) and average  
202 precipitation (blue line) are identical in Fig. 5. This result illustrates that the trend of water area change  
203 is consistent with that of average precipitation in the last thirty years.

204

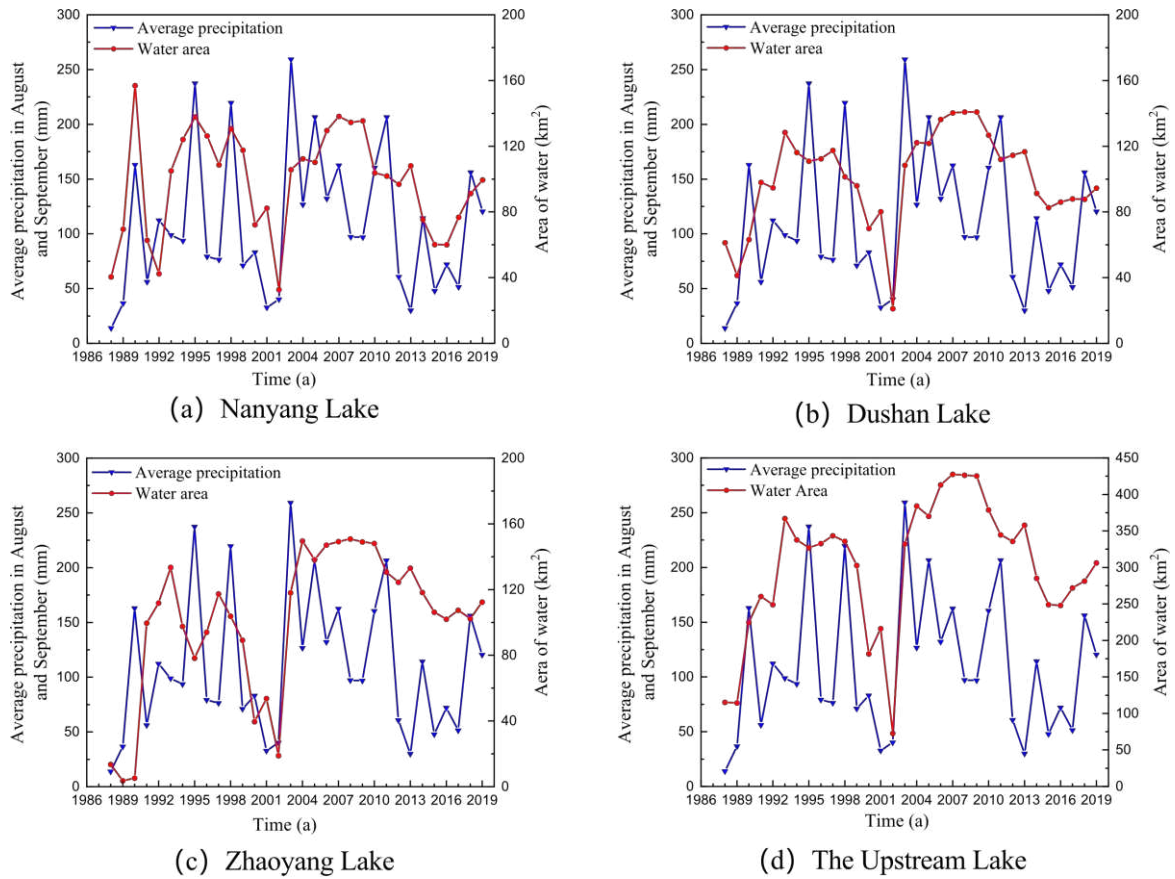


**Fig. 5 The trends of water area and average precipitation**

Therefore, it seems that underground mining in Jining and Tengbei coal fields has barely influence on the lake water area, instead, the water area change is related to the precipitation. However, the water area may be affected by the extension of underground mining to the lake. The total overlapping area of these two coal fields and the lake is  $398\text{km}^2$ , which is about 66% of the lake area. According to estimate, the subsidence volume of the lake bottom will be  $1.94 \times 10^9 \text{ m}^3$  after accomplish mining of two coal fields, but the lake storage capacity is only  $9.03 \times 10^8 \text{ m}^3$ , namely that most of the lake water will flow into the subsidence area, and the shallow water may no longer exist. Finally, this phenomenon can make a significant reduction in the water area.

### Analysis of RSEI indexes

According to the weights of four RSEI indexes (Table 1), the average RSEI increased from 0.583 to 0.632 between 1988 and 2009 (increased by 8.4%). However, the average RSEI decreased from 0.632 to 0.584 between 2009 and 2019 (decreased by 7.59%). RSEI appears a trend of the slow rise and then a sharp decline in this research area. This trend illustrates that the ecological environment

222 gets better and then gets worse. Moreover, PC1 loads of wet and FVC have a positive influence on the  
 223 ecological environment, but PC1 loads of NDBSI and LST have a negative influence on the ecological  
 224 environment (positive number: beneficial; negative number: harmful). The contributions of wet and  
 225 FVC show a reduced trend, but that of NDBSI and LST appear to a rising trend. These trends illustrate  
 226 vegetation coverage and construction land have a significant effect on the ecological environment, and  
 227 then the decline of vegetation coverage and increase of construction land make the ecological  
 228 environment worse.

229

230

**Table 1 Statistics of factor indicators and Remote Sensing Ecological Index**

Indexes	1988		1998		2009		2019	
	Average	PC1 load						
Wet	0.546	0.182	0.679	0.179	0.630	0.181	0.662	0.153
FVC	0.719	0.574	0.747	0.581	0.729	0.563	0.691	0.461
NDBSI	0.568	-0.551	0.560	-0.543	0.493	-0.572	0.366	-0.669
LST	0.338	-0.412	0.388	-0.402	0.433	-0.542	0.405	-0.631
RESI	0.583		0.587		0.632		0.584	

231

### 232 **Dynamic changes of ecological environment**

233 RSEI is divided into five levels for the change analysis of ecological environment: Poor (0~0.2),  
 234 Fair (0.2~0.4), Moderate (0.4~0.6), Good (0.6-0.8), Excellent (0.8~1.0) (Table 2).

235

236

**Table 2 Ecological environment classification**

RSEI Level	Description
Poor (0~0.2)	Severe natural ecological conditions, prominent ecological environmental problems, and extremely fragile ecological functions.
Fair (0.2~0.4)	Less vegetation coverage, fewer species, obvious ecological environmental problems, fragile ecological functions, and obvious factors limiting human activities.

---

Moderate (0.4~0.6)	Moderate vegetation coverage, general biodiversity, general natural ecological conditions, certain ecological environmental problems, and relatively fragile ecological functions.
Good (0.6~0.8)	Relatively high vegetation coverage, relatively abundant biodiversity, relatively good natural ecological condition, relatively stable ecological function, and certain ecological environmental problems.
Excellent (0.8~1.0)	High vegetation coverage, relatively abundant biodiversity, superior natural ecological condition, high ecosystem carrying capacity, stable ecosystem, and strong self-regulation ability.

---

237

238       According to the information of RESI change, the ecological environment of the east is generally  
239 worse than that of the west from 1988 to 2019 (Fig. 6). The main reason may low mountains and hills  
240 and serious soil erosion exist in the northeast (Ge et al. 2012). In the recent thirty years, the ecological  
241 environment of the northeast is better than before, which is related to afforestation and other beneficial  
242 activities of improving soil erosion. In addition, underground mining activities exist in the coal fields  
243 of the southeast for many years (Fig. 7), which can make surface subsidence of some areas. The surface  
244 subsidence can reduce the original covers of farmland, grassland, and woodland (Liang 2014; Meng  
245 and Dong 2019), and then cause a series of environmental problems. The level of ecological  
246 environment changes from excellent to fair or poor, ecological environmental problems and ecological  
247 function are more fragile. The ecological environment of the western area is better than that of the  
248 eastern area, but some poor areas appear an expansion trend in the western area. This phenomenon is  
249 probably caused by an increase in urban construction land (Liu et al. 2020).

250

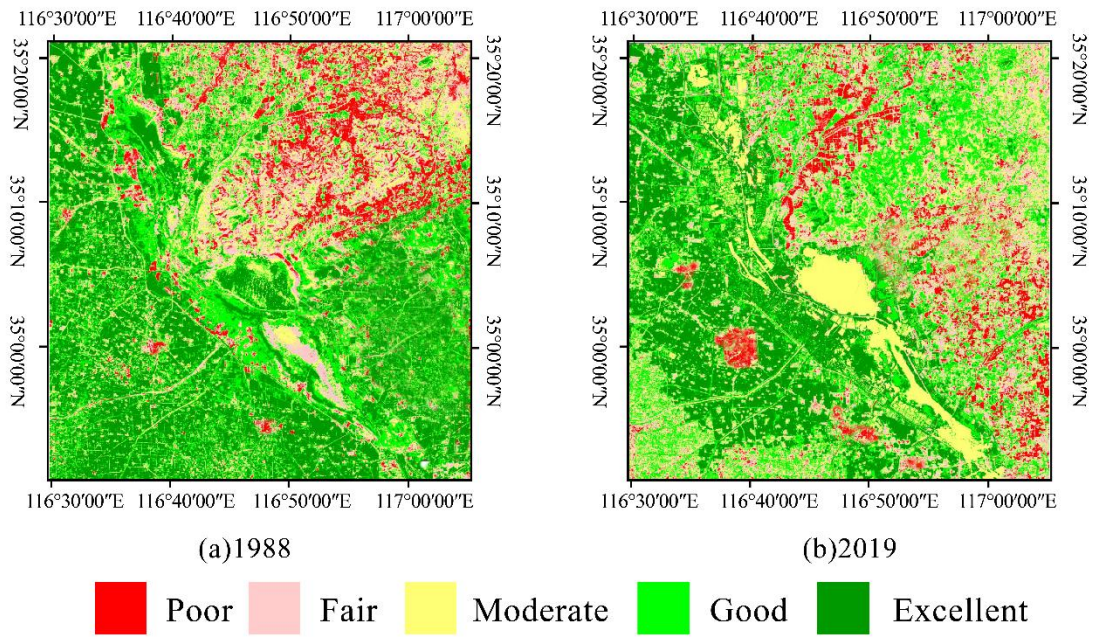


**Fig. 6 RSEI classification of the upstream Nansi lake**

Moreover, the ecological environment level of the lake grades from excellent or good to moderate. Underground mining activity is probably the main reason, three mines including Binhu, Xin'an, and Huxi mines (Fig. 7 and Table 3) implement mining activity under the lake. Therefore, mining activity is detrimental to biodiversity, ecological environment, and ecological function.

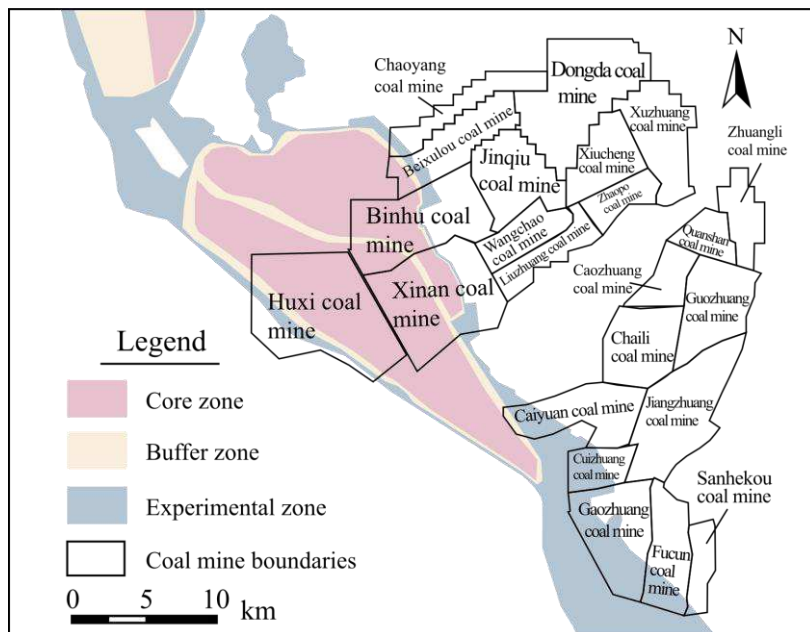


**Fig. 7 Distribution of mines around the upstream Nansi lake**

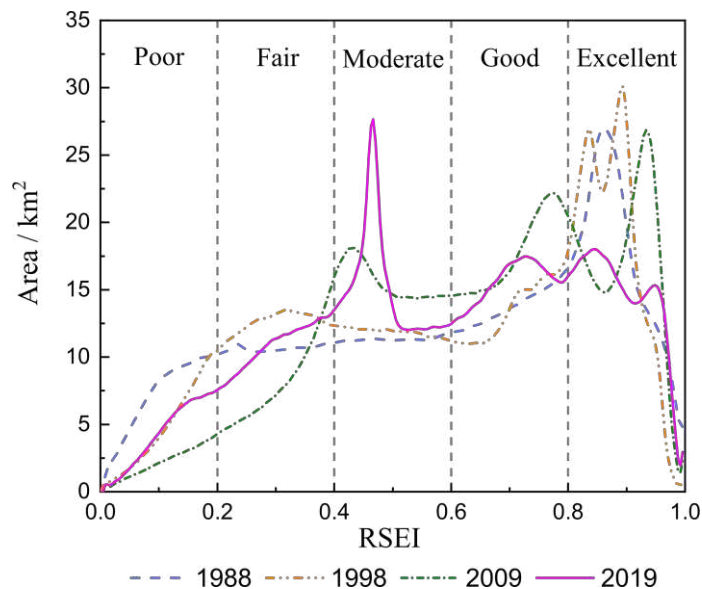
**Table 3 Overview of some mines in the research area**

Coal Field	Mine	Location relationship with the lake	Production time (year)	Design production capacity (1×10 <sup>4</sup> t/year)
Tengbei	Binhu	lakeside and under the lake	2005	1.10
	Xin'an	lakeside and under the lake	1998	3.53
	Huxi	lakeside and under the lake	2001	0.90
	Beixulou	lakeside and under the lake	1996	0.45
	Chaoyang	lakeside	2003	0.45
	Jinqiu	lakeside	2005	0.45
	Wangchao	lakeside	1994	0.30
	Liuzhuang	lakeside	1993	0.60
	Dongda	other	1995	0.45
Zhaopo	other	1991	0.50	
Tengbei	Cuizhuang	lakeside and under the lake	1993	0.60
	Gaozhaung	lakeside and under the lake	1997	3.20
	Fucun	lakeside and under the lake	1998	2.70
	Sanhekou	lakeside and under the lake	1992	0.60
	Caiyuan	lakeside and under the lake	1982	0.30
	Jiangzhuang	lakeside	1988	1.50
	Chaili	lakeside	1964	1.80

The RSEI result of 2019 is less than that of other years in the excellent level, and then the maximum appears in the moderate level, which is higher than that of other years (Fig. 8). In addition, the excellent level area decreases by 18.0% from 1988 to 2019. The good level area increases significantly in 2009 but decreases by 103.713 km<sup>2</sup> in 2019 compared to 2009 (Table 4). The trend of the moderate level area is similar to the good level, the decreased area is inapparent in 2019. The fair level area is maximum in 1998, and the area of 2019 is basically similar to 1988. The trend of poor

270 level area decreases from 1988 to 2009, and then the area increases by 101.782 km<sup>2</sup> between 2009 and  
 271 2019. Compared with 2009, the ecological quality of 2019 is worse. The reason for this change is due  
 272 to large-scale underground mining.

273



274

275

276

277

**Fig. 8 RSEI variation of the upstream Nansi lake**

**Table 4 Area of each ecological level and proportion**

RSEI Level	1988		1998		2009		2019	
	Area (km <sup>2</sup> )	Proportion (%)						
Poor (0~0.2)	352.660	11.558	231.710	7.594	106.156	3.479	207.938	6.815
Fair (0.2~0.4)	540.141	17.703	641.314	21.019	408.193	13.379	551.358	18.071
Moderate (0.4~0.6)	575.793	18.872	606.455	19.877	794.147	26.028	772.188	25.308
Good (0.6~0.8)	693.689	22.736	686.372	22.496	894.654	29.322	790.941	25.923
Excellent (0.8~1.0)	888.834	29.131	885.265	29.014	847.967	27.792	728.692	23.883

278

279

## 280 Conclusions

281 The remote sensing is applied to monitor the change of ecological environment in Nansi lake, and  
 282 the lake area is extracted by the SVM classifier of spectral and geometric texture information.

283 Moreover, four indexes of RSEI (greenness, humidity, dryness, and heat) are used to assess ecological  
284 environment quality with the PCA analysis method, which can avoid artificial subjective defects.

285 The change of the lake water area has little relation with underground mining but is related to the  
286 annual precipitation. According to estimate, the subsidence volume of the lake bottom will be  $1.94 \times 10^9$   
287  $\text{m}^3$  after accomplish mining of Tengnan and Tengbei coal fields, but the lake storage capacity is only  
288  $9.03 \times 10^8 \text{ m}^3$ , namely that most of the lake water will flow into the subsidence area, and the shallow  
289 water may no longer exist.

290 The area of deteriorating ecological environment is located in Tengnan and Tengbei coal fields.  
291 Vegetation coverage decreases (reduction of greenness and wetness; increase of dryness and heat) due  
292 to surface subsidence, gangue, and drainage. On the one hand, the deteriorating ecological quality of  
293 the lake area is mainly affected by mining activities including Huxi, Xin'an, and Binhu coal mines.  
294 The deteriorating ecological quality of the non-lake area is mostly influenced by Jinqiu, Wangchao,  
295 and Dongda coal mines. On the other hand, the area of improved ecological environment is located in  
296 the northeastern hilly area, which attributes the success to afforestation and other beneficial activities  
297 of improving soil erosion.

298 Finally, coal mines need to apply more environmentally friendly mining method for protecting the  
299 lake ecological environment, and actively participate in ecological restoration. Moreover, the coal  
300 mines from the natural reserve may be closed or limited to the mining boundary.

301

## 302 **Acknowledgments**

303 The authors are grateful to the Alexander von Humboldt Foundation for supporting this research  
304 team (CHN/1101176STP), National Research and Development Project (2016YFC0501105), and  
305 China Coal Technology & Engineering Group Project (2018-TD-MS052).

306

## 307 **Ethical Approval**

308 The manuscript does not involve animal and human experiments, so ethical approval is not  
309 applicable.

310

## 311 **Consent to Participate**

312 All the authors agree to participate in this research.

313

314 **Consent to Publish**

315 All the authors agree to publish the manuscript research.

316

317 **Authors Contributions**

318 Hu Liu: writing, calculation, and visualization

319 Yan Jiang: funding support, writing- reviewing and editing

320 Rafal Misa: model research, modification of the text, and discussion

321 Junhai Gao: project support, and scientific advice

322 Mingyu Xia: remote sensing data processing

323 Axel Preusse: providing scientific advice and reviewing

324 Anton Sroka: providing scientific advice and reviewing

325 Yue Jiang: providing research plan, remote sensing data processing, writing- reviewing and editing

326

327 **Funding**

328 This research work was financially supported by the Alexander von Humboldt Foundation  
329 (CHN/1101176STP), National Research and Development Project (2016YFC0501105), and China  
330 Coal Technology & Engineering Group Project (2018-TD-MS052).

331

332 **Availability of data and materials**

333 All data generated or analysed during this study are included in this manuscript.

334

335 **Conflict of Interest**

336 The authors declare no conflict of interest.

337

338 **References**

339 China MEE (2015) Technical Criterion for Ecosystem Status Evaluation vol HJ 192—2015. China Environmental  
340 Press, Beijing (in Chinese)

341 Crist EP (1985) A TM Tasseled Cap equivalent transformation for reflectance factor data. Remote Sensing of

342 Environment 17:301-306. [https://doi.org/10.1016/0034-4257\(85\)90102-6](https://doi.org/10.1016/0034-4257(85)90102-6)

343 Den K, Tan Z, Jiang Y, Dai H, Shi Y, Xu L (2015) Deformation Monitoring and Subsidence Engineering. China  
344 University of Mining and Technology Press, Xuzhou (in Chinese)

345 Du Q, Fowler JE (2007) Hyperspectral Image Compression Using JPEG2000 and Principal Component Analysis.  
346 IEEE Geoscience and Remote Sensing Letters 4:201-205.<https://doi.org/10.1109/LGRS.2006.888109>

347 Ge XL, Liu J, Wang RQ (2012) The Comparison between the Historical and Current Vegetation in Nansi Lake Area.  
348 Advanced Materials Research 518-523:5180-5184.[https://doi.org/10.4028/www.scientific.net/AMR.518-](https://doi.org/10.4028/www.scientific.net/AMR.518-523.5180)  
349 523.5180

350 Gold C, Sollich P (2003) Model selection for support vector machine classification. Neurocomputing 55:221-249.  
351 [https://doi.org/10.1016/S0925-2312\(03\)00375-8](https://doi.org/10.1016/S0925-2312(03)00375-8)

352 Huang C, Wylie B, Yang L, Homer C, Zylstra G (2002) Derivation of a tasselled cap transformation based on Landsat  
353 7 at-satellite reflectance. International Journal of Remote Sensing 23:1741-  
354 1748.<https://doi.org/10.1080/01431160110106113>

355 Jiang Y, R.MISA, Li P, Yuan X, A.Sroka, Jiang Y (2019) Summary and Development of Mining Subsidence Theory.  
356 Metal Ming 10:1-7.<https://doi.org/10.19614/j.cnki.jsks.201910001> (in Chinese)

357 Kratzsch H (1974) Mining subsidence engineering. Springer-Verlag, Berlin

358 Li M, Jiang M (2003) Effect of Coal-mining to Environment in Nansihu Area. Shandong Land and Resources 05:28-  
359 31 (in Chinese)

360 Liang CL (2014) NDVI Changes of the Nansi Lake in Shandong Province of China. Advanced Materials Research  
361 919-921:1659-1662.<https://doi.org/10.4028/www.scientific.net/AMR.919-921.1659>

362 Ma L, Guo J, Liu W, Zhang D, Yu Y (2019) Water Conservation when Mining Multiple, Thick, Closely-Spaced Coal  
363 Seams: A Case Study of Mining Under Weishan Lake. Mine Water and the Environment 38:643-  
364 657.<https://doi.org/10.1007/s10230-019-00610-8>

365 Meng L, Dong J (2019) LUCC and Ecosystem Service Value Assessment for Wetlands: A Case Study in Nansi Lake,  
366 China. Water 11:1597.<https://doi.org/10.3390/w11081597>

367 Nichol J (2005) Remote sensing of urban heat islands by day and night. Photogrammetric Engineering & Remote  
368 Sensing 71:613-621.<https://doi.org/10.14358/PERS.71.5.613>

369 Reddish D, Whittaker B (1989) Subsidence: occurrence, prediction and control. Elsevier, Amsterdam

370 Rikimaru A, Roy P, Miyatake S (2002) Tropical forest cover density mapping. Tropical ecology 43:39-47

371 Shu K (1992) Experiment and research on coal mining under Weishanhu Lake. Coal Science and Technology 07:44-

372 49.<https://doi.org/10.13199/j.cst.1992.07.45.shuksh.013> (in Chinese)

373 Sobrino JA, Jiménez-Muñoz JC, Paolini L (2004) Land surface temperature retrieval from LANDSAT TM 5. *Remote*

374 *Sensing of Environment* 90:434-440. <https://doi.org/10.1016/j.rse.2004.02.003>

375 Sui WH, Xu ZM Risk Assessment for Coal Mining Under Sea Area. In, Berlin, Heidelberg, 2013. *New Frontiers in*

376 *Engineering Geology and the Environment*. Springer Berlin Heidelberg, pp 199-

377 202.[https://doi.org/10.1007/978-3-642-31671-5\\_35](https://doi.org/10.1007/978-3-642-31671-5_35)

378 Teng Y, Gao D, Zhu W (2012) *Coal Mining under Water*. China Coal Industry Publishing House, Beijing (in Chinese)

379 Todd SW, Hoffer RM (1998) Responses of spectral indices to variations in vegetation cover and soil background.

380 *Photogrammetric Engineering and Remote Sensing* 64:915-921

381 Wang W, Liu X, Wang Y, Guo X, Lu S (2016) Analysis of point source pollution and water environmental quality

382 variation trends in the Nansi Lake basin from 2002 to 2012. *Environmental Science and Pollution Research*

383 23:4886-4897.<https://doi.org/10.1007/s11356-015-5625-x>

384 Xu H (2008) A new index for delineating built-up land features in satellite imagery. *International Journal of Remote*

385 *Sensing* 29:4269-4276.<https://doi.org/10.1080/01431160802039957>

386 Xu ZM, Sui WH Statistical Prediction of Overburden Failure Due to Coal Mining Under Sea Area. In, Berlin,

387 Heidelberg, 2013. *New Frontiers in Engineering Geology and the Environment*. Springer Berlin Heidelberg, pp

388 255-258.[https://doi.org/10.1007/978-3-642-31671-5\\_46](https://doi.org/10.1007/978-3-642-31671-5_46)

389 Zhang D, Sui W, Liu J (2018) Overburden Failure Associated with Mining Coal Seams in Close Proximity in

390 Ascending and Descending Sequences Under a Large Water Body. *Mine Water and the Environment* 37:322-

391 335.<https://doi.org/10.1007/s10230-017-0502-0>

392 Zhou ZC, Shanguan ZP, Zhao D (2006) Modeling vegetation coverage and soil erosion in the Loess Plateau Area

393 of China. *Ecological Modelling* 198:263-268. <https://doi.org/10.1016/j.ecolmodel.2006.04.019>

# Figures

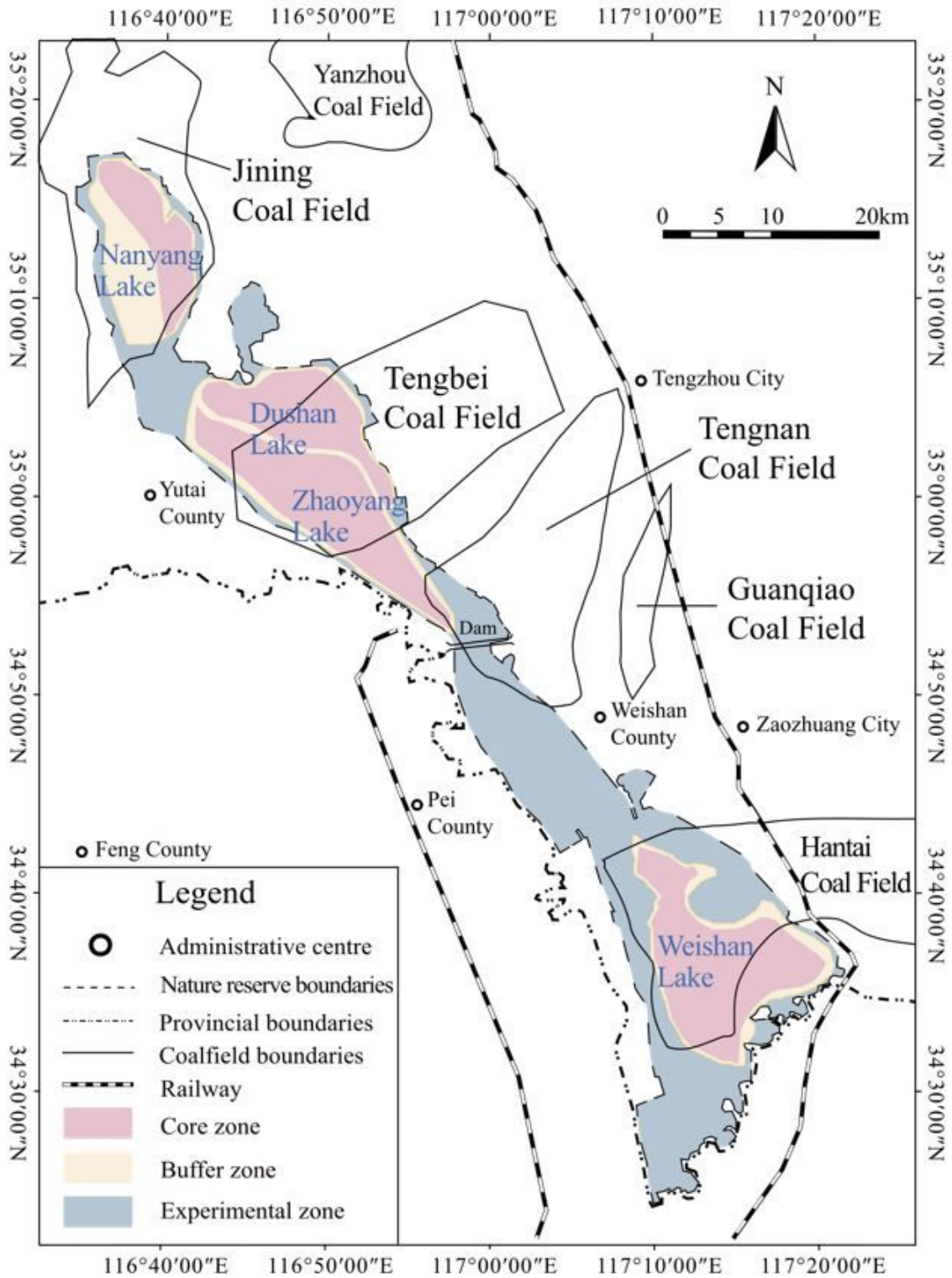


**Figure 1**

Distribution of Nansi lake nature reserve and coal resources Note: The designations employed and the presentation of the material on this map do not imply the expression of any opinion whatsoever on the part of Research Square concerning the legal status of any country, territory, city or area or of its

authorities, or concerning the delimitation of its frontiers or boundaries. This map has been provided by the authors.

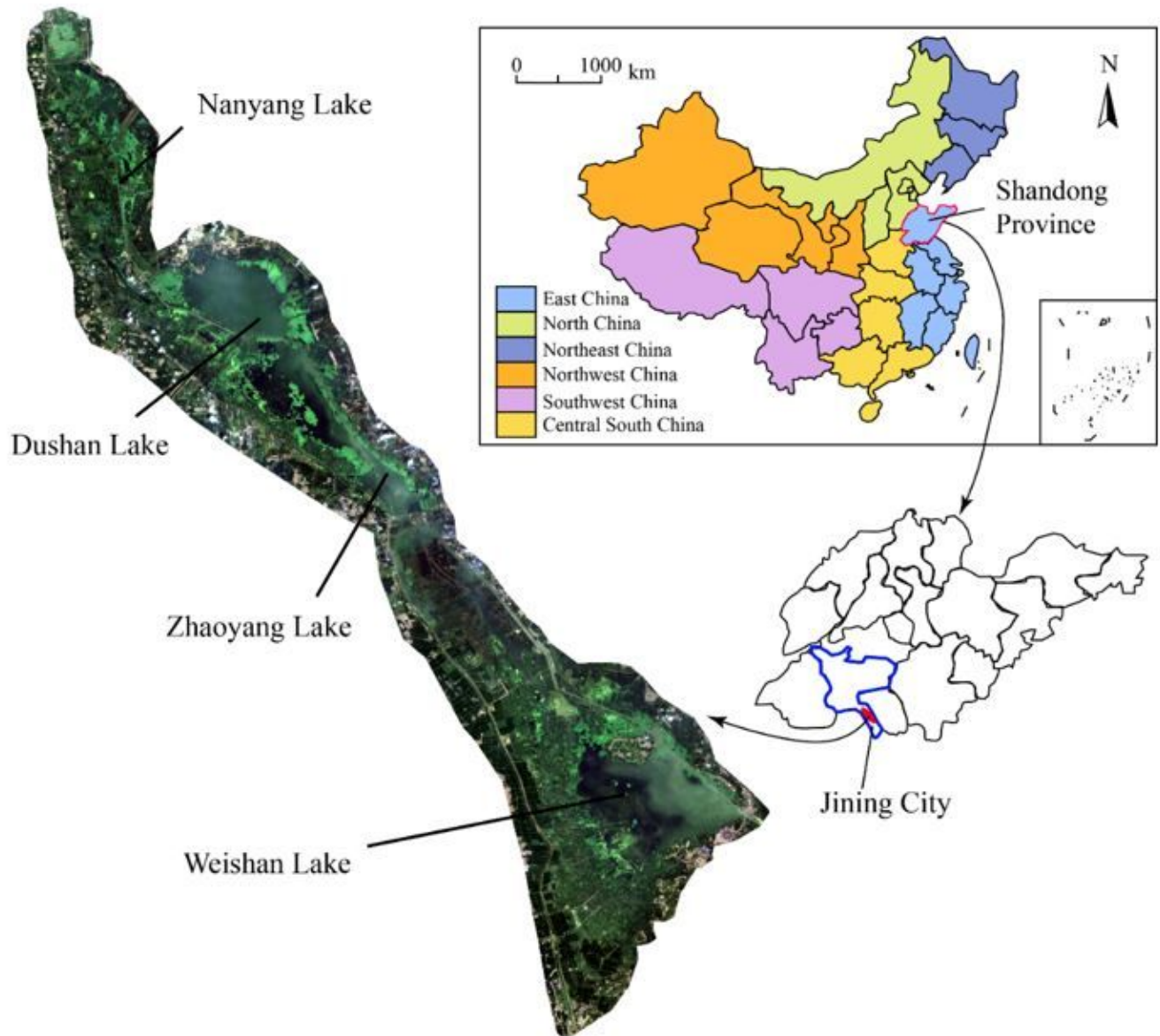


**Figure 2**

Location of Nansi Lake (2019 Landsat-8 OLI image) Note: The designations employed and the presentation of the material on this map do not imply the expression of any opinion whatsoever on the part of Research Square concerning the legal status of any country, territory, city or area or of its authorities, or concerning the delimitation of its frontiers or boundaries. This map has been provided by the authors.

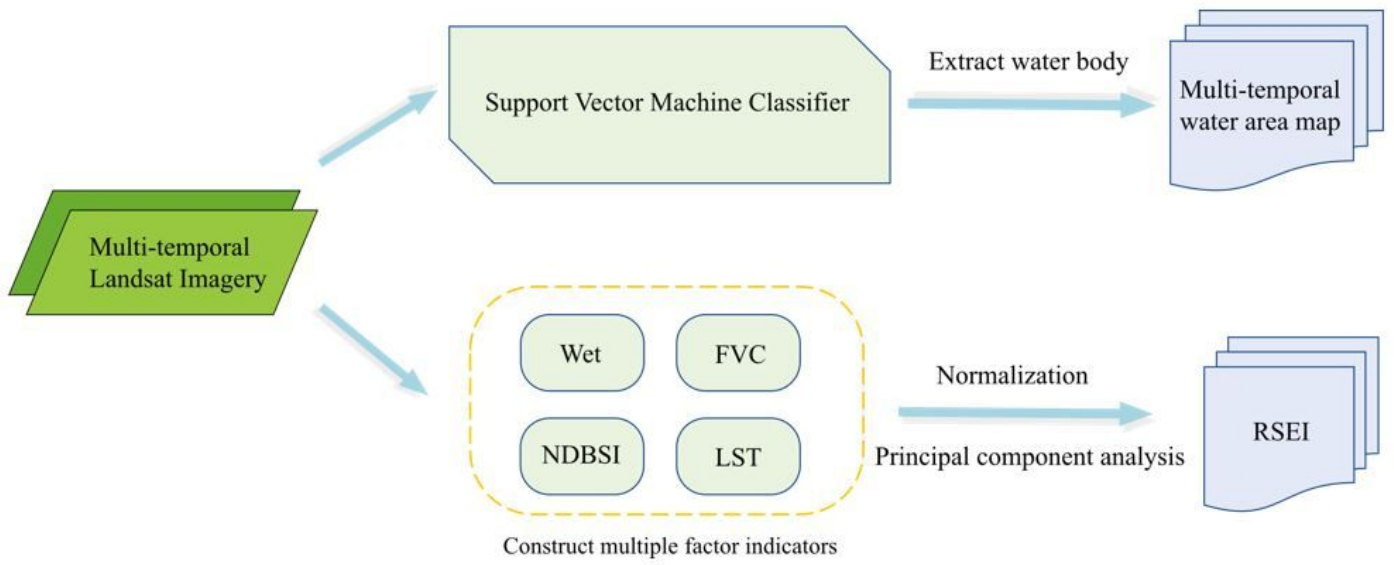


**Figure 3**

Research method route

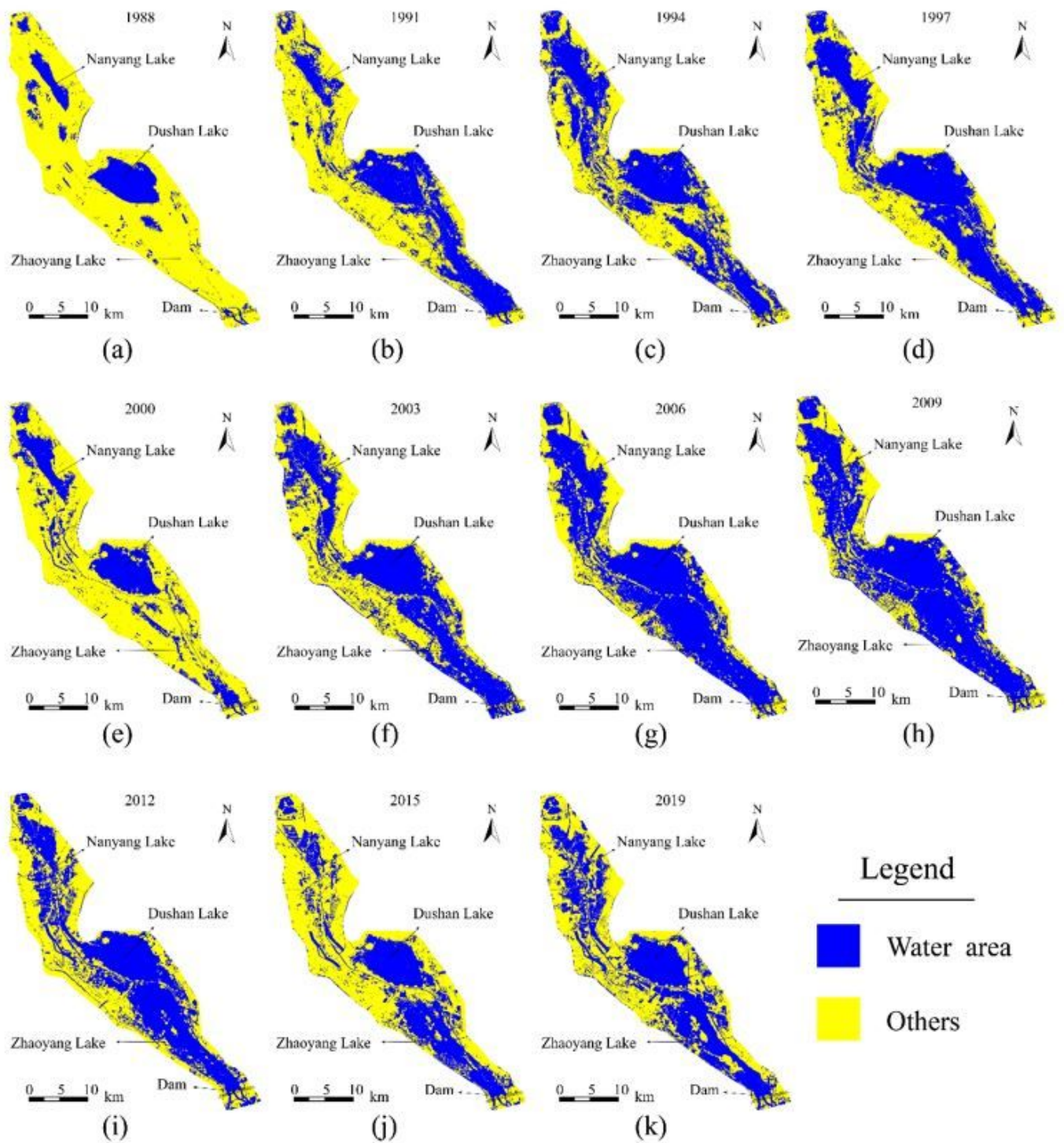
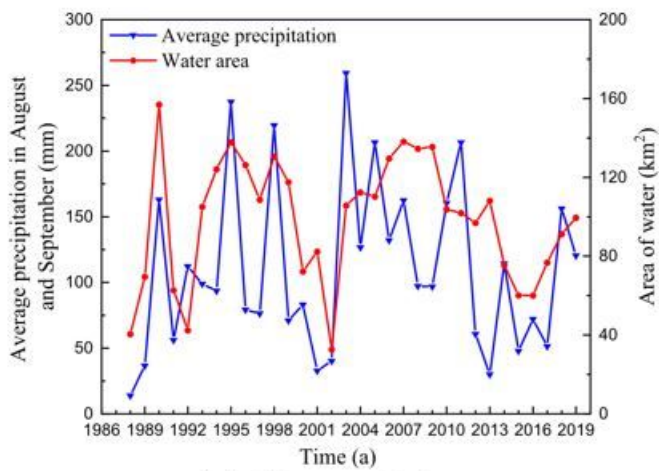
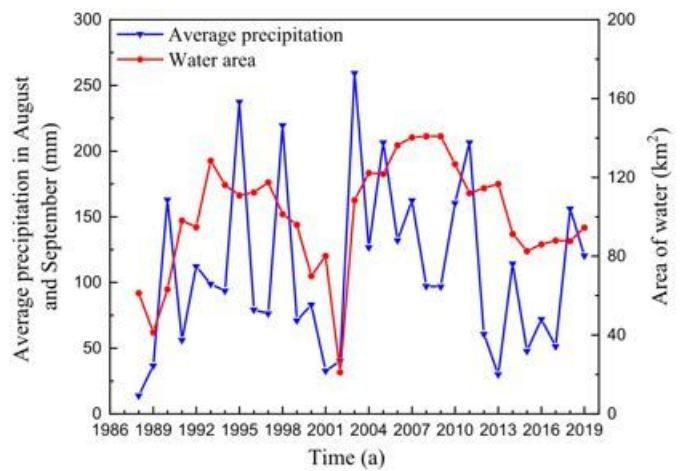


**Figure 4**

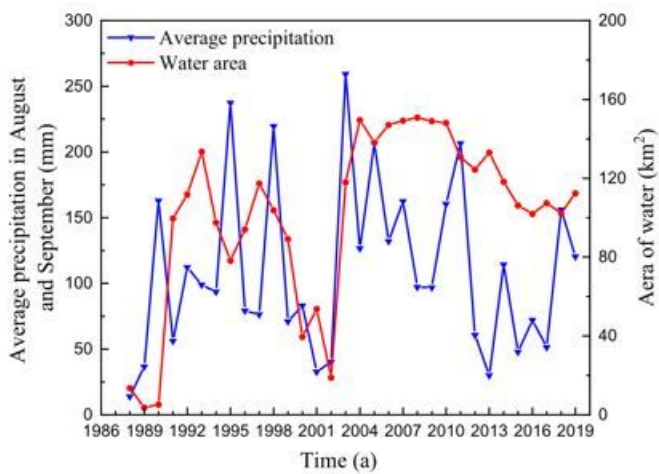
Variation characteristics of the upstream Nansi lake Note: The designations employed and the presentation of the material on this map do not imply the expression of any opinion whatsoever on the part of Research Square concerning the legal status of any country, territory, city or area or of its authorities, or concerning the delimitation of its frontiers or boundaries. This map has been provided by the authors.



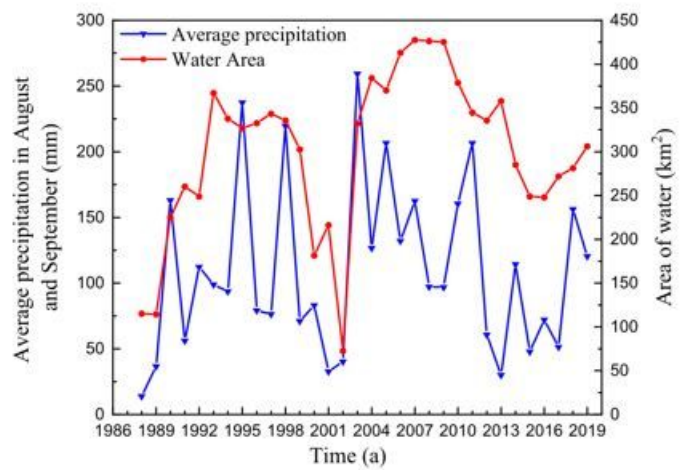
(a) Nanyang Lake



(b) Dushan Lake



(c) Zhaoyang Lake



(d) The Upstream Lake

Figure 5

The trends of water area and average precipitation

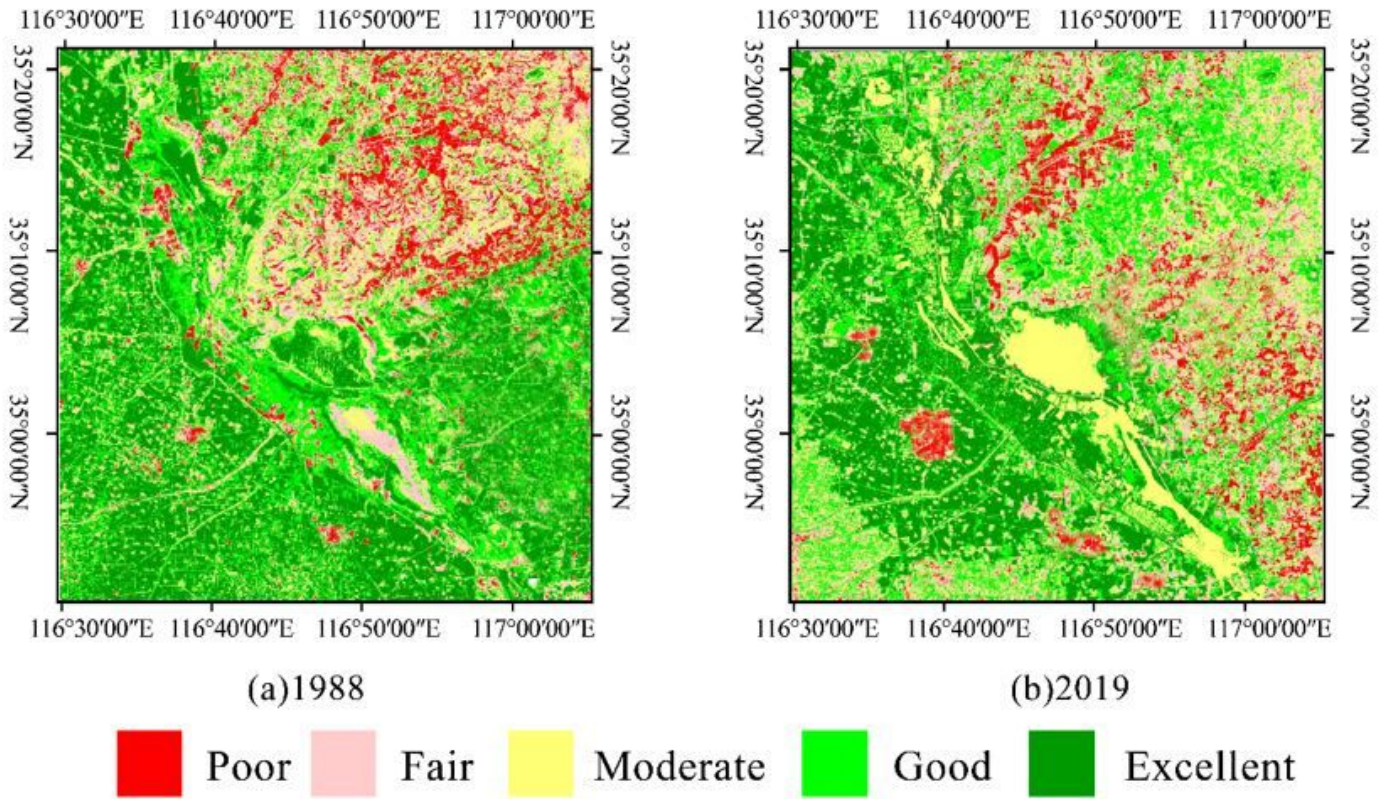


**Figure 6**

RSEI classification of the upstream Nansi lake Note: The designations employed and the presentation of the material on this map do not imply the expression of any opinion whatsoever on the part of Research Square concerning the legal status of any country, territory, city or area or of its authorities, or concerning the delimitation of its frontiers or boundaries. This map has been provided by the authors.

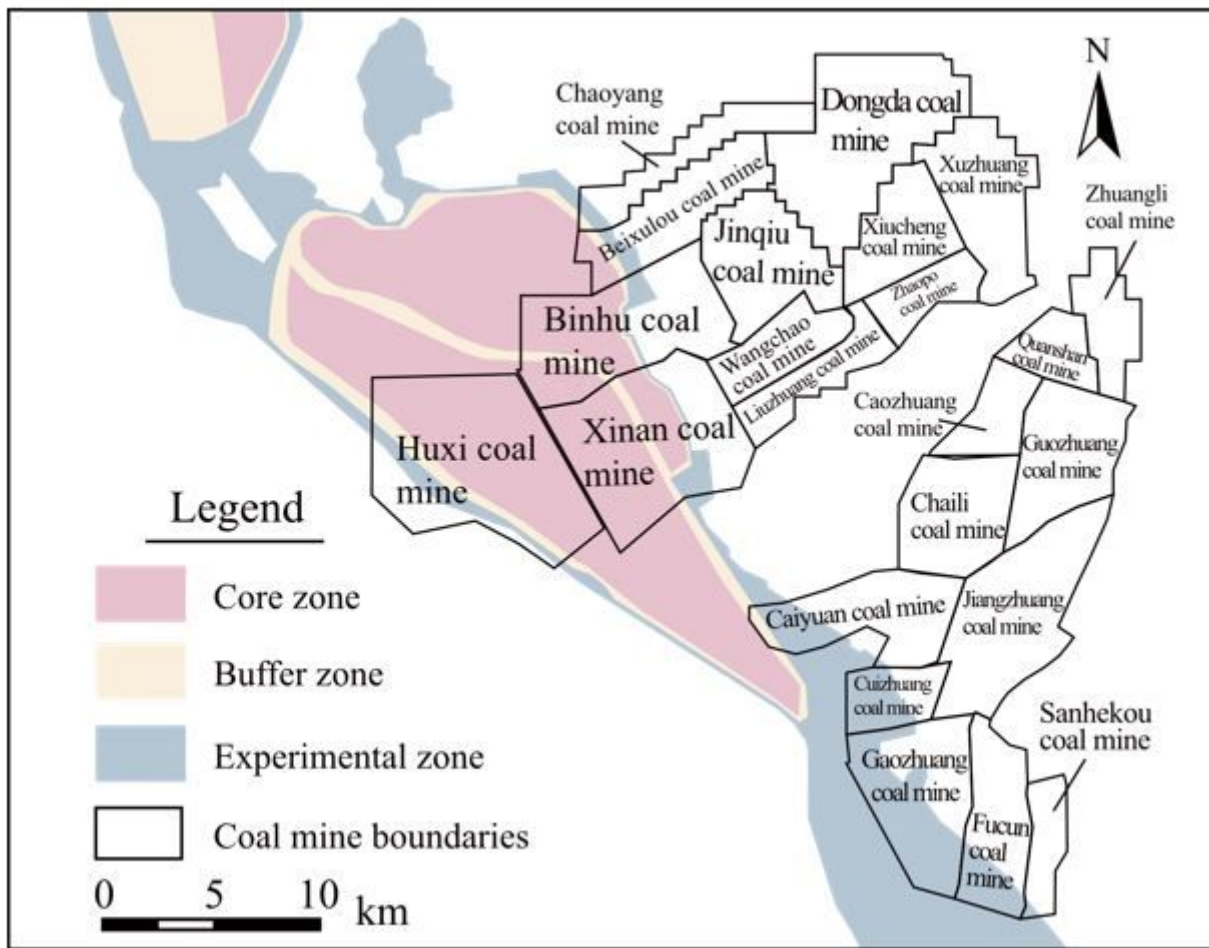


**Figure 7**

Distribution of mines around the upstream Nansi lake Note: The designations employed and the presentation of the material on this map do not imply the expression of any opinion whatsoever on the part of Research Square concerning the legal status of any country, territory, city or area or of its authorities, or concerning the delimitation of its frontiers or boundaries. This map has been provided by the authors.

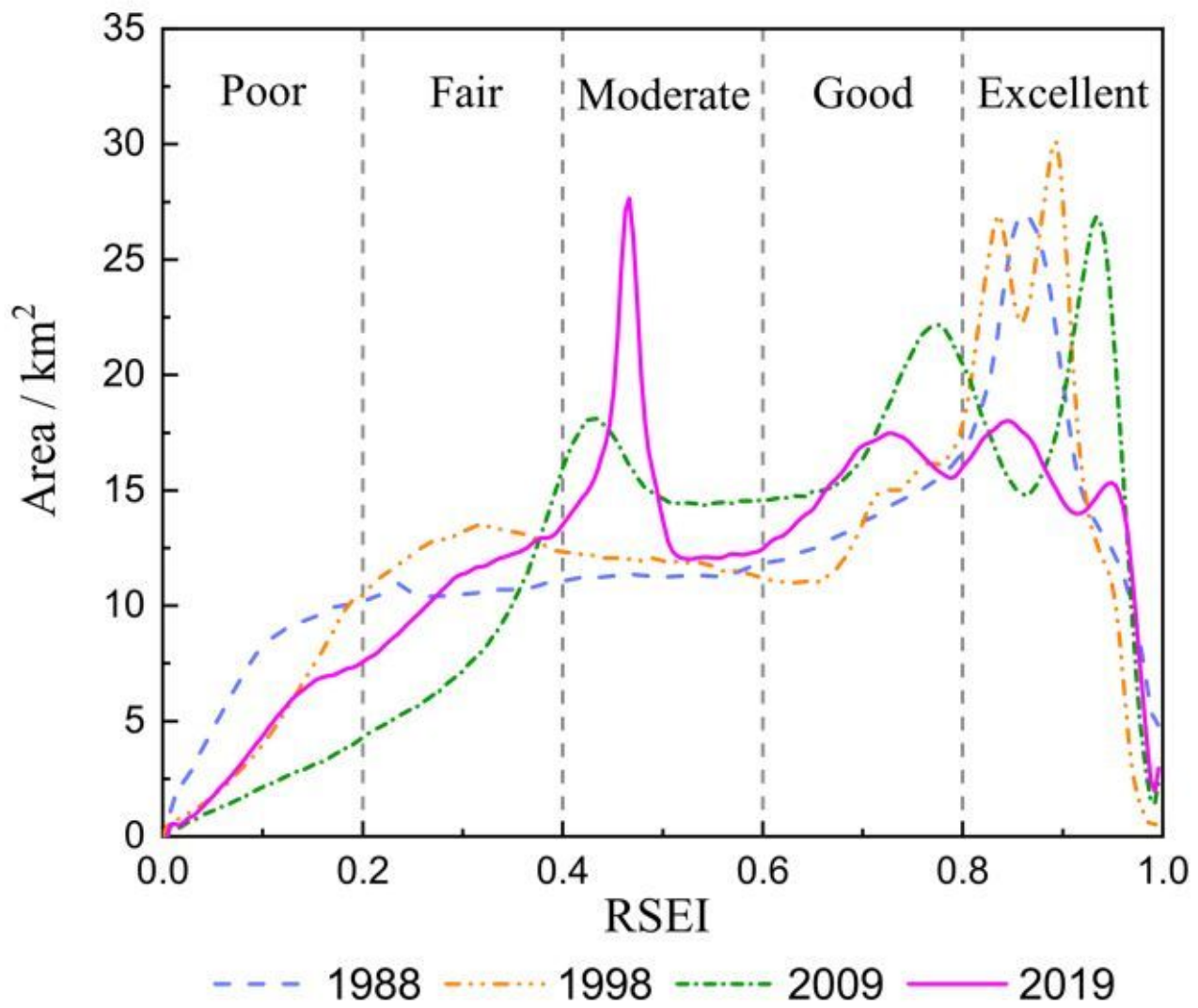


Figure 8

RSEI variation of the upstream Nansi lake